OFFICE OF NAVAL RESEARCH

Contract Nonr 562(10)

NR-064-406

Technical Report No. 63

DESIGN OF THIN-WALLED TORISPHERICAL AND TORICONICAL PRESSURE VESSEL HEADS

by

R. T. Shield and D. C. Drucker

DIVISION OF APPLIED MATHEMATICS

BROWN UNIVERSITY

PROVIDENCE, R. I.

C11-63

July 1960

C11-63

DESIGN OF THIN-WALLED TORISPHERICAL AND TORICONICAL PRESSURE VESSEL HEADS*

by R. T. Shield** and D. C. Drucker***

Summary

The failure under hydrostatic test of a large storage vessel designed in accordance with current practice stimulated earlier analytical studies. This paper gives curves and a table useful for the design and analysis of the knuckle region of a thin torispherical or toriconical head of an unfired cylindrical vessel. A simple but surprisingly adequate approximate formula is presented for the limit pressure, np^D, at which appreciable plastic deformations occur:

$$\frac{np^D}{\sigma_o} = (0.33 + 5.5\,\frac{r}{D})\frac{t}{L} + 28(1 - 2.2\,\frac{r}{D})(\frac{t}{L})^2 - 0.0006,$$

where p^D is the design pressure, σ_o is the yield stress of the material, and n is the factor of safety. The thickness t of the knuckle region is assumed uniform. Upper and lower bound calculations were made for ratios of knuckle radius r to cylinder diameter D of 0.06, 0.08, 0.10, 0.12, 0.14, and 0.16, and ratios of spherical cap radius L to D of 1.0, 0.9, 0.8,

---

* The results presented in this paper were obtained in the course of research sponsored by the Office of Naval Research under Contract Nonr 562(10) with Brown University.

** Professor of Applied Mathematics, Brown University.

*** Professor of Engineering, Brown University.

0.7, and 0.6. Toriconical heads may be designed or analyzed closely enough by interpreting φ_o of the Table as the complement of the half angle of the cone.

Introduction

The design of pressure vessels requires the long experience distilled into the ASME Code to avoid overlooking many important factors. In principle, the most straightforward of the difficult problems is the design of an unreinforced knuckle region of uniform thickness in an unfired pressure vessel subjected to interior pressure. This topic is discussed at length in the Code and it might well be expected that little remained to be resolved. Surprisingly, analytical studies[1,2] stimulated by reports of a failure under hydrostatic test demonstrated conclusively that the thickness required by the Code is inadequate for a range of designs. This range is one of small pressures and consequently of vessels whose wall

---

1. G. D. Galletly has studied elastic behavior in "Torispherical Shells - A Caution to Designers", Journal of Engineering for Industry, ASME, v. 81, 1959, pp. 51-62, and "On Particular Integrals for Toroidal Shells Subjected to Uniform Internal Pressure", Journal of Applied Mechanics, ASME, v. 25, 1958, pp. 412-413.

2. D. C. Drucker and R. T. Shield have studied plastic behavior in "Limit Strength of Thin Walled Pressure Vessels with an ASME Standard Torispherical Head", Proceedings Third U. S. National Congress of Applied Mechanics, Brown University, 1958, ASME, pp. 665-672, and "Limit Analysis of Symmetrically Loaded Thin Shells of Revolution", Journal of Applied Mechanics, ASME, v. 26, 1959, pp. 61-68.

thickness is small compared with the knuckle radius as well as the radius of the vessel itself. It did not, in all likelihood, engage the serious attention of the framers of the Code who were concerned primarily with pressures exceeding several hundred pounds per square inch. At these higher pressures, a sharply curved knuckle would have a radius which is not very large compared with the wall thickness and so the knuckle would not be flexible and weak.

A design of adequate strength must provide a reasonable factor of safety against reaching the limit pressure, the pressure at which significantly large plastic deformation will take place. Many additional practical matters as well must be taken into account in the design. Among these are corrosion allowance, thinning allowance, and joint efficiency. They will not be considered here except by implication in the designation of the limit pressure as np^D where n is a factor of safety and p^D is the design or working pressure.

The limit pressure is especially significant in a cold environment for those steels which are prone to brittle fracture. Appreciable plastic deformation below the transition temperature is almost certain to initiate a brittle fracture. Above this rather ill-defined transition temperature, the shape of a vessel of ductile material will be able to change sufficiently to carry the pressure without catastrophic failure. The pressure simply cold forms the head to a quite different but much better shape for containing pressure.

A Qualitative Discussion of the Behavior of Pressure Vessels

A thin-walled vessel under interior pressure is most efficient when it can carry the pressure as a membrane in biaxial tension. However, the shape required for this desirable membrane behavior[3] has a height of head H = 0.26D which often appears too large from the fabrication or space utilization point of view. Torispherical heads are employed to reduce H appreciably but they cannot act in biaxial tension; they must carry circumferential compression in the knuckle and also resist bending. Their load carrying capacity as pure membranes (no moment resistance), shown in the Table as $p^{M}D/2\sigma_{o}t$ and plotted on some of the graphs at t/D = 0, is extremely low. Actually, a very thin shell acting as a membrane would buckle in circumferential compression.

As the pressure builds up, it tends to force the spherical cap outward along the axis and the meridional membrane tensions pull the toroidal knuckle inward toward the axis. If the torus wall is thick enough to avoid buckling but thin compared with the radius of the knuckle, and the material does not work-harden, a plastic hinge circle will form at B, Fig. 1, to permit the central region of the knuckle to compress in the circumferential direction and bend inwards. A hinge circle will form at C in the spherical cap and the third hinge circle A usually forms in the cylinder. The entire knuckle region

---

3. R. A. Struble, "Biezeno Pressure Vessel Heads", Journal of Applied Mechanics, ASME, v. 23, 1956, pp. 642-645.

between A and C is plastic because inward motion of appreciable extent means plastic contraction of the circumference. A thin-walled sharply curved knuckle region is far weaker than the main part of the spherical cap or the cylindrical portion of the vessel. On the other hand, if the torus wall is not so thin compared with the knuckle radius, the knuckle region is stiff and strong and acts somewhat like a stiffening ring at the junction of a spherical cap and a cylinder. The ASME Code which requires very little variation of $np^{D}D/\sigma_{o}t$ with t/D apparently contains the implicit assumption that ordinarily the resistance to inward motion of the knuckle region is adequately high. Although true for vessels designed to carry large pressure, the assumption is not valid for many storage vessels and other low pressure containers. For these thin-walled vessels there is a large variation of the value of $np^{D}D/2\sigma_{o}t$ with t/D as shown in Figs. 2-5. On the other hand, the dotted lines for values of $np^{D}D/2\sigma_{o}t$ greater than unity show that for less sharply curved knuckles and for relatively thick knuckles, the knuckle region is stronger than the main cylindrical part of the vessel.

Design Curves and Formula

The upper and lower bound theorems of limit anaylsis and design[4] were used to calculate the limit pressure. Therefore, even within the usual idealizations of the theory of plasticity,

4. D. C. Drucker, W. Prager, and H. J. Greenberg, "Extended Limit Design Theorems for Continuous Media", Quarterly of Applied Mathematics v. 9, 1952, pp. 381-389.

the exact answer is bounded rather than determined directly. Curves are plotted in Figs. 2 and 3 for $p^U D/2\sigma_o t$, the upper (unsafe) values computed for $np^D D/2\sigma_o t$, and in Figs. 4 and 5 for $p^L D/2\sigma_o t$, the lower (oversafe) values. The designer then can make an independent judgment of the appropriate values to use.

However, if moderate accuracy is good enough or if a preliminary design is sought, Fig. 6 should prove a very helpful alternative. An approximate plot of t/D vs. H/D for discrete values of np^D/σ_o, it gives a clear picture of the penalty to be paid for the advantage of decreasing the axial length of the vessel. The agreement with the mean of the upper and lower bound calculations, also shown on Fig. 6, varies with r/D and L/D but to a much smaller extent than might be expected.

Remarkably good agreement with the limit calculations can be achieved through use of the variable t/L which is of prime importance in the ASME Code. The excellent fit of the simple formula

$$\frac{np^D}{\sigma_o} = (0.33 + 5.5\,\frac{r}{D})\frac{t}{L} + 28(1 - 2.2\,\frac{r}{D})(\frac{t}{L})^2 - 0.0006$$

is illustrated in Fig. 7, a plot of t/L vs. np^D/σ_o for two values of r/D. The relatively minor variation with L/D is also a feature of the Code. However, the Code calls for a linear variation of t/L with increasing pressure and there is no way of adjusting a straight line to the proper curves without being unsafe or far too safe. The lack of safety is all too

evident in Fig. 8, a plot of the formula for discrete values of r/D, which permits the designer to select t/L for a given pressure or to check the pressure carrying capacity of an existing design. Again the designer is urged to return to Figs. 2-5 to obtain upper and lower bounds on his factor of safety if he is forced to design with a very small margin.

The Appendix contains detailed information on the basis and the methods of calculation of Figs. 2-5. It supplements the discussion contained in the earlier papers[2] and is not complete in itself. In essence, the Tresca or maximum shearing stress criterion of yield is employed and the yield surface for the shell is a cut off parabolic approximation to the exact shape for a symmetrically loaded cylindrical shell.

Toriconical Heads

The values of t/L and np^D/σ_o plotted for a given torus apply equally well to torispherical and to toriconical heads. The Table can be used to obtain the appropriate interpolated value of L/D for Figs. 2-5 if desired. The angle φ_o is the complement of the torus angle and therefore the complement of the half angle of the cone.

Appendix

The equations of equilibrium for the various portions of the vessel, cylinder, torus and sphere, are given in the references of footnote 2. The term involving the circumferential bending moment M_θ is omitted from the equations of equilibrium for the torus and the sphere as M_θ has little influence in carrying load for thin shells at sections not too near the axis of symmetry. The meridional bending moment M_φ is similarly omitted but its derivative is retained.

As M_θ is considered as a passive moment in the curved portions of the shell as well as in the cylinder, full use of M_φ and the meridional and circumferential force resultants N_φ and N_θ in carrying the internal pressure p is obtained by using the yield condition on N_φ, N_θ, M_φ for the cylinder. In order to approximate to this yield condition or surface, the circumscribing surface consisting of a parabolic cylinder with four cut off planes is used[2]. In the region of interest between the hinge circles A, B, C of Fig. 1, N_φ is tensile and N_θ is compressive. For this region to be at yield, the parabolic prism yield surface requires

$$N_\varphi - N_\theta = \sigma_o t \ , \quad |M_\varphi| \leq \tfrac{1}{4} \sigma_o t^2 \{1 - (N_\varphi/\sigma_o t)^2\} \ . \qquad (1)$$

It is assumed that at the hinge circles A and C in the cylinder and the sphere, M_φ attains its largest negative value and at hinge circle B in the torus, M_φ attains its largest positive

value. The shear force Q is zero at the hinge circles. Under these conditions the equations of equilibrium can be integrated to provide the distribution of N_θ, N_φ, M_φ and Q in the plastic region.

It is found that in the cylinder,

$$M_\varphi = -\frac{1}{4}\sigma_o t^2\{1-(\frac{pD}{4\sigma_o t})^2\} + \frac{1}{2}\sigma_o \frac{t}{D}(2+\frac{pD}{2\sigma_o t})(x_o-x)^2 , \qquad (2)$$

$$Q = -\sigma_o \frac{t}{D}(2+\frac{pD}{2\sigma_o t})(x_o-x) , \qquad (3)$$

where x measures distance from the junction with the torus and x_o defines the location of the hinge circle A. In the torus,

$$\frac{M_\varphi}{r\sigma_o t} = \frac{1}{4}\frac{t}{r}\{1-(\frac{pD}{2\sigma_o t})^2 \frac{(R+r\sin\varphi_m)^2}{D^2\sin^2\varphi_m}\} - \frac{pR}{2\sigma_o t}\frac{[1-\cos(\varphi-\varphi_m)]}{\sin\varphi_m}$$
$$+ \frac{r}{R}\cos\varphi\,[k(\varphi_m)-k(\varphi)] + \log\{\frac{R+r\sin\varphi}{R+r\sin\varphi_m}\} , \qquad (4)$$

$$\frac{Q}{\sigma_o t} = \frac{pR}{2\sigma_o t}\frac{\sin(\varphi_m-\varphi)}{\sin\varphi_m} + \frac{r}{R}\sin\varphi\,[k(\varphi)-k(\varphi_m)] , \qquad (5)$$

where

$$k(\varphi) = \int_{\varphi_o}^{\varphi} \frac{R\,d\varphi}{R+r\sin\varphi} = \frac{2R}{(R^2-r^2)^{1/2}}\left[\tan^{-1}\{\frac{r+R\tan\frac{1}{2}\varphi}{(R^2-r^2)^{1/2}}\}\right]_{\varphi_o}^{\varphi} , \qquad (6)$$

φ is the angle between the meridional normal and the axis of the shell and φ_m is the location of the hinge circle B. In the sphere, with the assumption that $\varphi - \varphi_o$ is small,

$$\frac{M_\varphi}{L\sigma_o t} = -\frac{1}{4}\frac{t}{L}\{1-(\frac{pL}{2\sigma_o t})^2\} + \frac{1}{2}(\varphi-\varphi_s)^2 , \qquad (7)$$

$$\frac{Q}{\sigma_o t} = \varphi - \varphi_s , \qquad (8)$$

where φ_s defines the location of the hinge circle C.

The four quantities p, φ_m, φ_s and x_o are determined from the conditions that M_φ and Q are continuous at the junctions of the cylinder and torus (x=0, $\varphi=\pi/2$) and the torus and sphere ($\varphi=\varphi_o$). These conditions can be written

$$(2 + \frac{pD}{2\sigma_o t})(\frac{x_o}{D})^2 = j(\varphi_m)(\frac{pD}{2\sigma_o t})^2 + a(\varphi_m)\frac{pD}{2\sigma_o t} + b(\varphi_m) , \quad (9)$$

$$(2 + \frac{pD}{2\sigma_o t})\frac{x_o}{D} = c(\varphi_m)\frac{pD}{2\sigma_o t} + d(\varphi_m) , \quad (10)$$

$$(\varphi_o-\varphi_s)^2 = \ell(\varphi_m)(\frac{pD}{2\sigma_o t})^2 + e(\varphi_m)\frac{pD}{2\sigma_o t} + f(\varphi_m) , \quad (11)$$

$$\varphi_o-\varphi_s = g(\varphi_m)\frac{pD}{2\sigma_o t} + h(\varphi_m) , \quad (12)$$

where the functions not previously defined are given by

$$a(\varphi_m) = -2\frac{rR}{D^2}\frac{(1-\sin\varphi_m)}{\sin\varphi_m} , \quad (13)$$

$$b(\varphi_m) = 2\frac{r}{D}\log\{\frac{R+r}{R+r\sin\varphi_m}\} + \frac{t}{D} , \quad (14)$$

$$c(\varphi_m) = \frac{R}{D}\cot\varphi_m , \quad (15)$$

$$d(\varphi_m) = -\frac{r}{R}[k(\pi/2) - k(\varphi_m)] , \quad (16)$$

$$e(\varphi_m) = -2\frac{rR}{LD}\frac{[1-\cos(\varphi_m-\varphi_o)]}{\sin\varphi_m} , \quad (17)$$

$$f(\varphi_m) = 2\frac{r^2}{LR}\cos\varphi_o k(\varphi_m) + 2\frac{r}{L}\log\{\frac{R+r\sin\varphi_o}{R+r\sin\varphi_m}\} + \frac{t}{L} , \quad (18)$$

$$g(\varphi_m) = \frac{R}{D}\frac{\sin(\varphi_m-\varphi_o)}{\sin\varphi_m} , \quad (19)$$

$$h(\varphi_m) = -\frac{r}{R}\sin\varphi_o\, k(\varphi_m) , \quad (20)$$

$$j(\varphi_m) = -\frac{1}{2}\frac{t}{D}\left\{\frac{1}{4} + \frac{(R+r\sin\varphi_m)^2}{D^2\sin^2\varphi_m}\right\}, \tag{21}$$

$$\ell(\varphi_m) = -\frac{1}{2}\frac{t}{L}\left\{\left(\frac{L}{D}\right)^2 + \frac{(R+r\sin\varphi_m)^2}{D^2\sin^2\varphi_m}\right\}. \tag{22}$$

Equations (9)-(12) were solved for $pD/2\sigma_o t$, φ_m, φ_s and x_o/D for given values of the parameters t/D, L/D and r/D which define the geometry of the vessel. The following values of the parameters were used:

t/D = 0.002, 0.004, 0.006, 0.008, 0.010, 0.012, 0.014,
L/D = 1.0, 0.9, 0.8, 0.7, 0.6,
r/D = 0.06, 0.08, 0.10, 0.12, 0.14, 0.16.

In the numerical method used, a trial value φ_m^a was chosen for φ_m and the functions of φ_m occurring on the right-hand sides of equations (9)-(12) were evaluated. By elimination of φ_o-φ_s between (11) and (12), a quadratic equation was obtained for $pD/2\sigma_o t$. The positive root of this equation was then substituted in (9) and (10) to give two values of $(x_o/D)^2$. The difference between these two values was evaluated and the procedure was repeated with another trial value φ_m^b for φ_m, and again the difference between the two values of $(x_o/D)^2$ was found. Linear interpolation between φ_m^a and φ_m^b was then used to give a better approximation to the true value of φ_m. The process was repeated until the magnitude of the difference between the two values of $(x_o/D)^2$ as provided by

(9) and (10) was less than 10^{-7}.

For a few of the thinner vessels (12 out of the 210 considered), the upper hinge circle A does not lie in the cylinder but is located in the torus and the analysis requires a straightforward modification. The details of this modification will not be given here.

The value of the pressure p obtained from equations (9)-(12) (or from the modified analysis) is the limit pressure p^U for the head with the parabolic yield surface. As this surface circumscribes the exact yield surface for the cylinder, p^U is an upper bound to the true limit pressure. The values of p^U are shown in Figs. 2 and 3. A lower bound $p^L = \lambda p^U$ is obtained by choosing the factor λ so that the stress points λN_φ, λN_θ, λM_φ lie within the yield surface for the cylinder for all sections of the plastic region. The factor is given by

$$\lambda = (P^2 - 4P + 12)/2(P^2 - 4P + 8) , \qquad (23)$$

where $P = p^U D/2\sigma_o t$, the critical section being the hinge circle A in the cylinder. The factor varies from 0.82 to 0.90 as P varies from 0.5 to 1.0, and the values of $p^L D/2\sigma_o t$ are given in Figs. 4 and 5. The average of the upper and lower bounds will be sufficiently close to the true limit pressure for practical purposes. Thus we put $np^D = (p^U + p^L)/2$, where p^D is the design pressure and n the factor of safety against collapse.

For a given thickness ratio t/D, the limit pressure

np^D increases as r/D increases and decreases as L/D increases. The ratio H/D of the height of the head to the diameter depends similarly on the ratios r/D, L/D, as can be seen from the Table. In Fig. 6, approximate curves for t/D versus H/D for constant values of np^D/σ_o are shown for the range $0.17 < H/D < 0.28$ covered by the ranges 0.06 to 0.16 for r/D and 0.7 to 1.0 for L/D. Actual points for $np^D/\sigma_o = 0.004$, 0.010, 0.016 and 0.022 are also shown for comparison with the approximate curves.

It was found that for a fixed value of r/D, the variation of np^D/σ_o with t/L is almost independent of the ratio L/D. For L/D = 0.7 and 0.8, the formula

$$\frac{np^D}{\sigma_o} = (0.33 + 5.5\,\frac{r}{D})\frac{t}{L} + 28(1 - 2.2\,\frac{r}{D})(\frac{t}{L})^2 - 0.0006 \qquad (24)$$

provides values of np^D/σ_o which are very close (e.g. within 3% for t/L = 0.010) to the values calculated from $np^D = (p^U+p^L)/2$. Formula (24) is also adequate for L/D = 1.0, 0.9 and 0.6 as can be seen from Fig. 7, in which the formula (24) is compared with the values calculated from $np^D = (p^U+p^L)/2$ for the cases r/D = 0.06 and 0.16. Comparison with the ASME Code for unfired pressure vessels is also made in Fig. 7. The ASME Code gives

$$\frac{p^D}{SE} = 2\,\frac{t}{L}/(M+0.2\,\frac{t}{L}) \ , \qquad (25)$$

where $M = \frac{1}{4}[3+(L/r)^{1/2}]$, S is the maximum allowable stress and E is the efficiency of the welded joints. For the present purposes, SE was taken to be σ_o/n.

Acknowledgement

The authors would like to thank Mrs. Lois Paul for her assistance with the computations.

TABLE

$\frac{L}{D}$	$\frac{r}{D}$	φ_o (deg.)	$\frac{H}{D}$	$\frac{pM_D}{2\sigma_o t}$	$\frac{L}{D}$	$\frac{r}{D}$	φ_o (deg.)	$\frac{H}{D}$	$\frac{pM_D}{2\sigma_o t}$
1.0	0.06	27.91	0.1694	0.064	0.9	0.06	31.59	0.1844	0.079
	0.08	27.16	0.1815	0.087		0.08	30.81	0.1957	0.108
	0.10	26.39	0.1937	0.111		0.10	30.00	0.2072	0.139
	0.12	25.58	0.2063	0.136		0.12	29.16	0.2188	0.171
	0.14	24.75	0.2190	0.163		0.14	28.27	0.2306	0.205
	0.16	23.88	0.2319	0.190		0.16	27.35	0.2427	0.240
0.8	0.06	36.48	0.2050	0.101	0.7	0.06	43.43	0.2353	0.134
	0.08	35.69	0.2152	0.139		0.08	42.64	0.2440	0.184
	0.10	34.85	0.2256	0.179		0.10	41.81	0.2528	0.238
	0.12	33.97	0.2360	0.221		0.12	40.93	0.2619	0.296
	0.14	33.06	0.2468	0.265		0.14	40.01	0.2710	0.357
	0.16	32.09	0.2577	0.312		0.16	39.02	0.2804	0.423
0.6	0.06	54.57	0.2869	0.185					
	0.08	53.87	0.2934	0.256					
	0.10	53.13	0.3000	0.333					
	0.12	52.34	0.3068	0.417					
	0.14	51.50	0.3136	0.507					
	0.16	50.60	0.3207	0.606					

$$H = L - (L-r)\cos\varphi_o$$

$$\sin\varphi_o = (\tfrac{1}{2} - \tfrac{r}{D})/(\tfrac{L}{D} - \tfrac{r}{D})$$

$$\frac{pM_D}{2\sigma_o t} = \frac{rD}{L(L-r)}$$

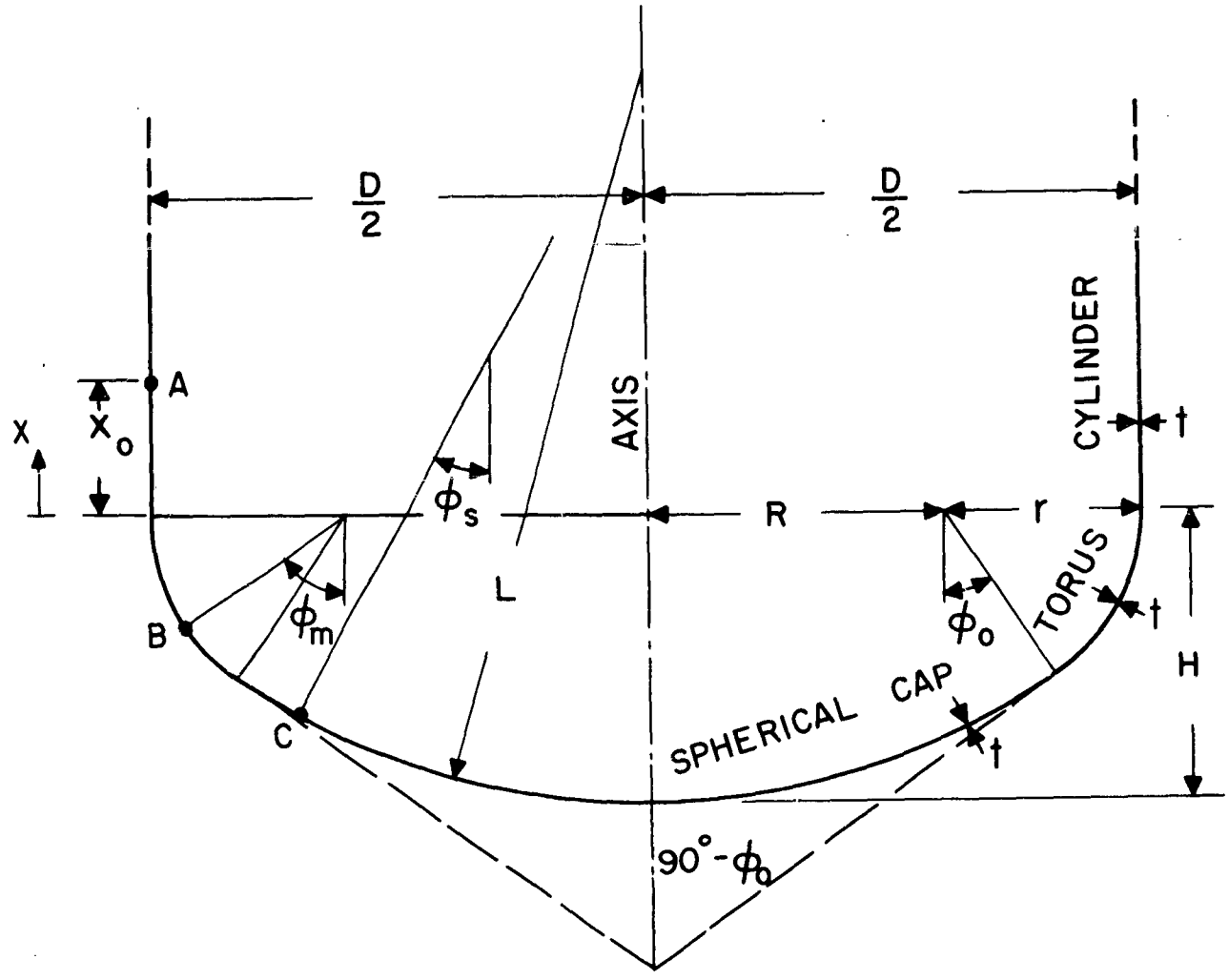

FIG. 1 TORISPHERICAL HEAD, SHOWING DIMENSIONS AND LOCATIONS OF HINGE CIRCLES A,B,C. (THE EQUIVALENT TORICONICAL HEAD IS SHOWN BY THE DASHED LINE WHICH IS TANGENT TO THE TORUS AT ITS LOWER END.)

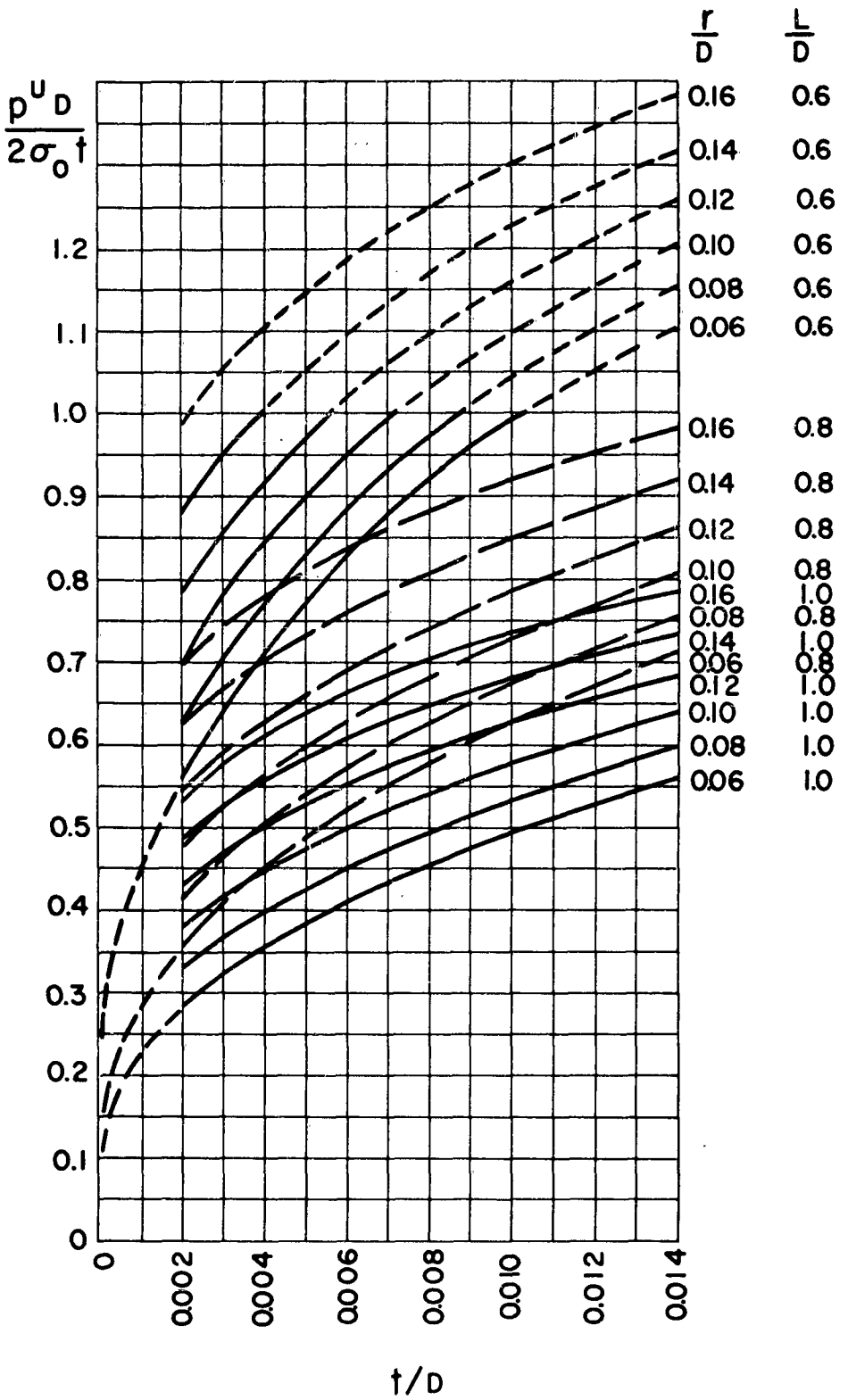

FIG. 2 UPPER (UNSAFE) BOUND ON LIMIT PRESSURE. L/D = 0.6, 0.8, 1.0

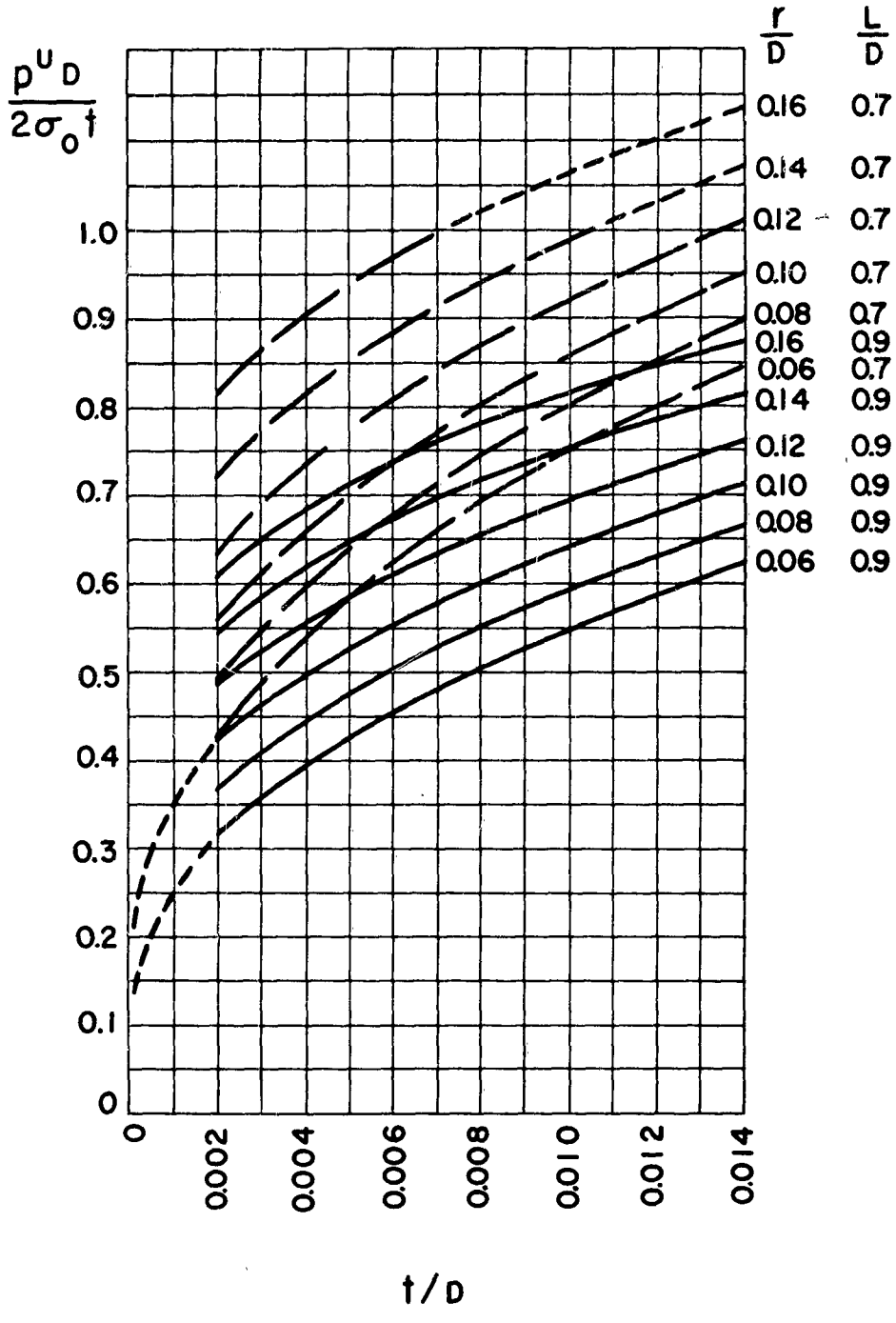

FIG. 3 UPPER (UNSAFE) BOUND ON LIMIT PRESSURE. L/D = 0.7, 0.9

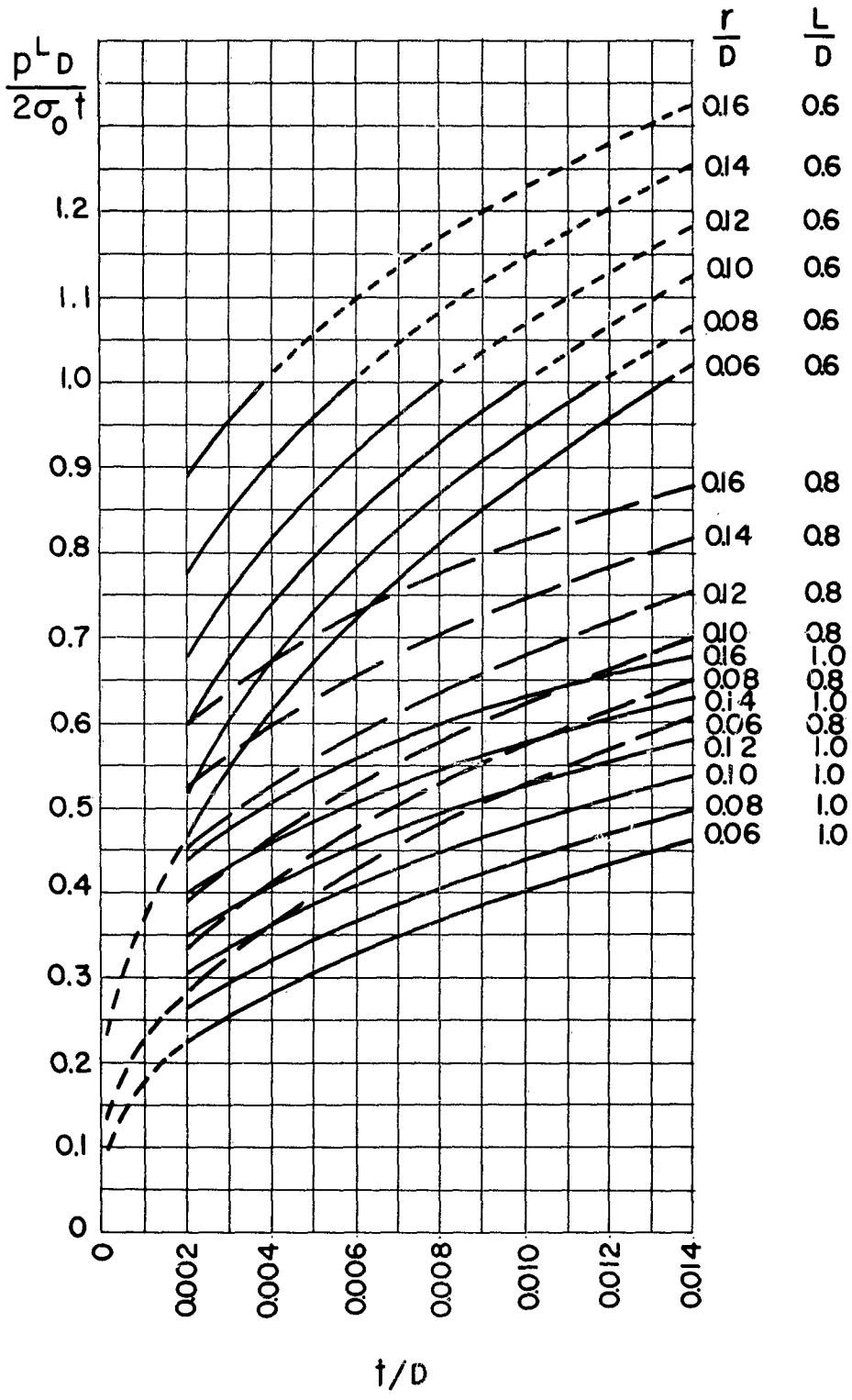

FIG. 4 LOWER (SAFE) BOUND ON LIMIT PRESSURE. L/D = 0.6, 0.8, 1.0

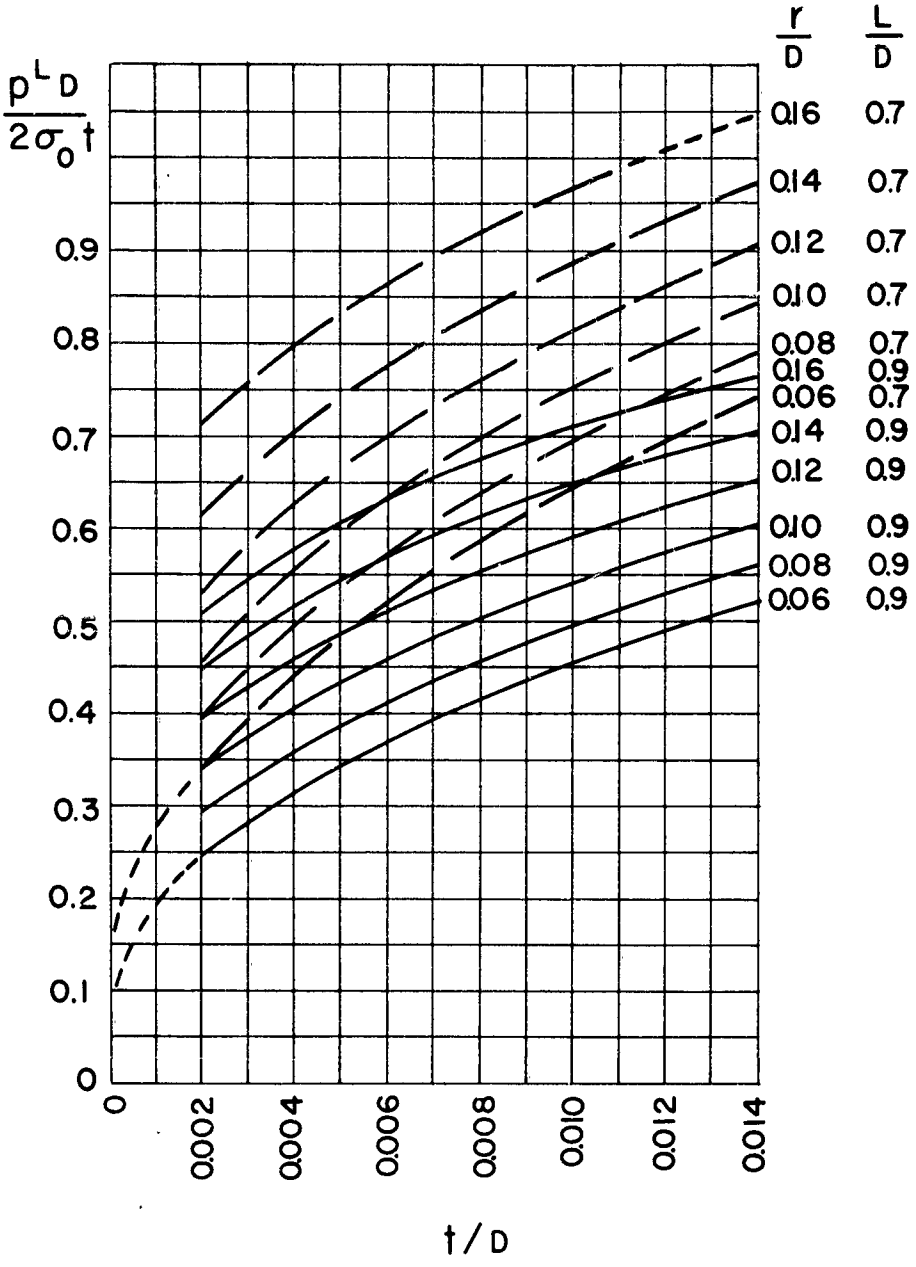

FIG. 5 LOWER (SAFE) BOUND ON LIMIT PRESSURE. L/D= 0.7, 0.9

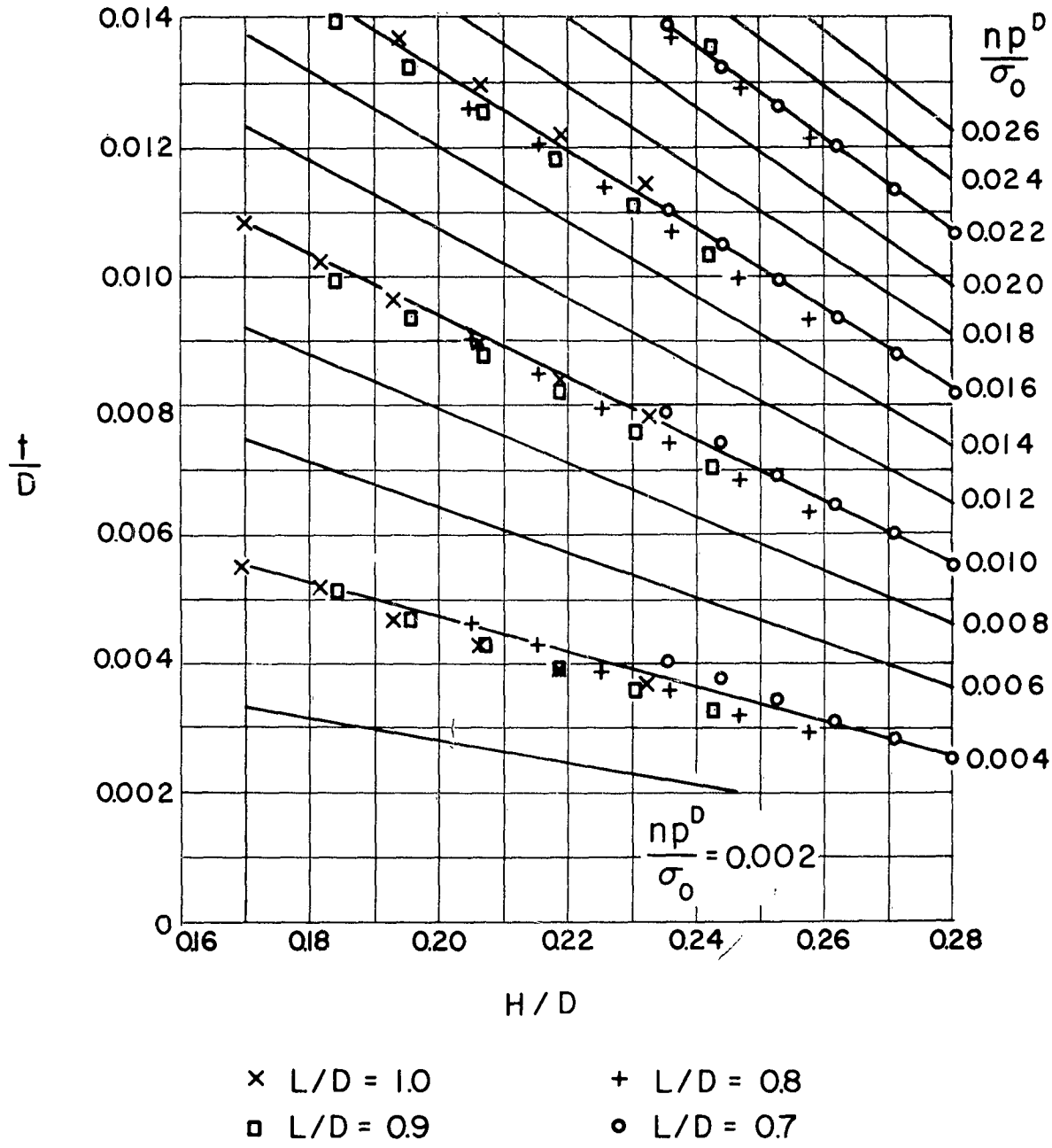

FIG. 6 APPROXIMATE CURVES FOR t/D VERSUS H/D FOR CONSTANT np^D/σ_0 (FOR L/D = 0.06, H/D VARIES FROM 0.29 TO 0.32)

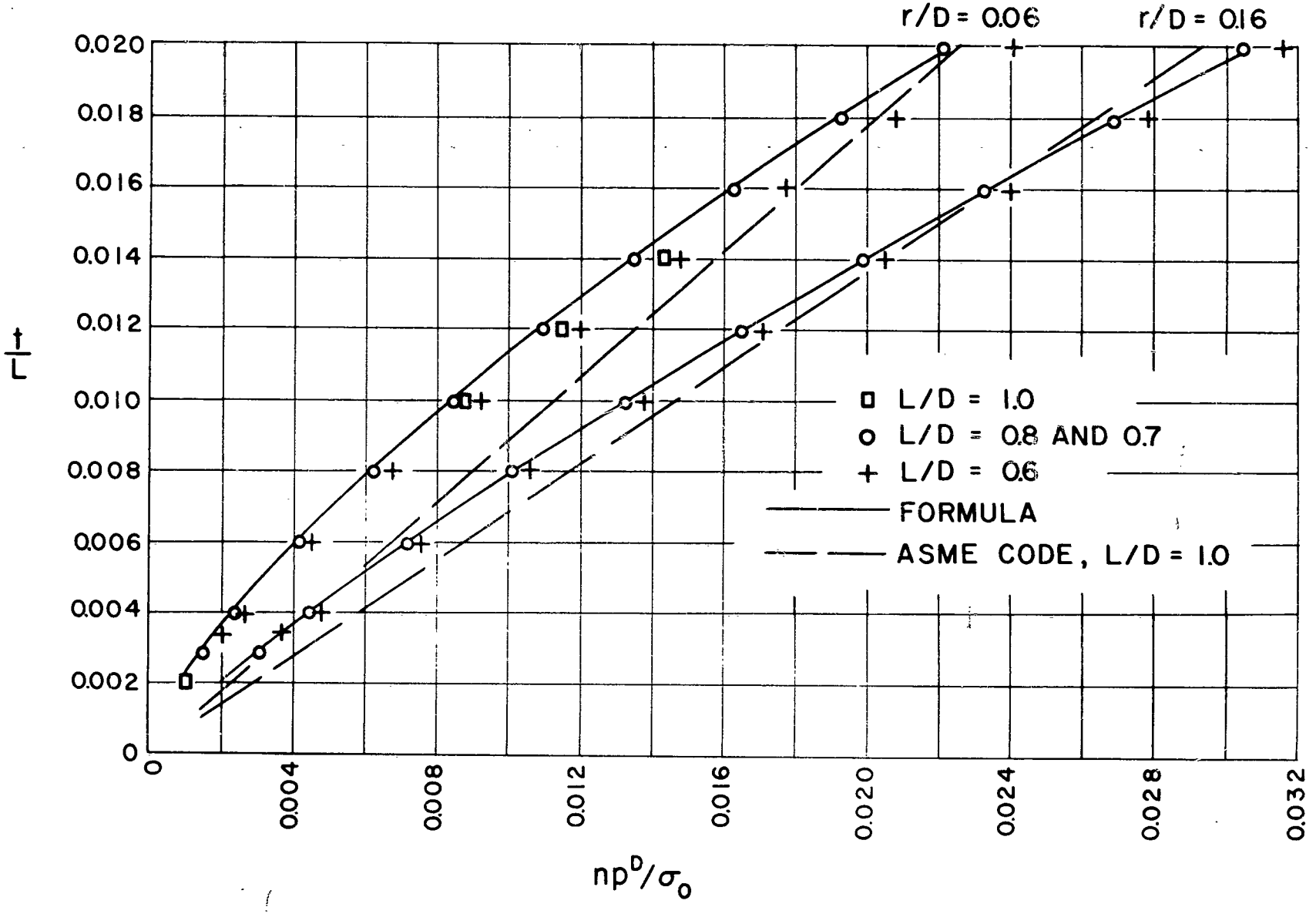

FIG. 7 COMPARISON OF FORMULA WITH AVERAGE OF UPPER AND LOWER BOUNDS AND WITH ASME CODE FOR r/D = 0.06 AND 0.16.

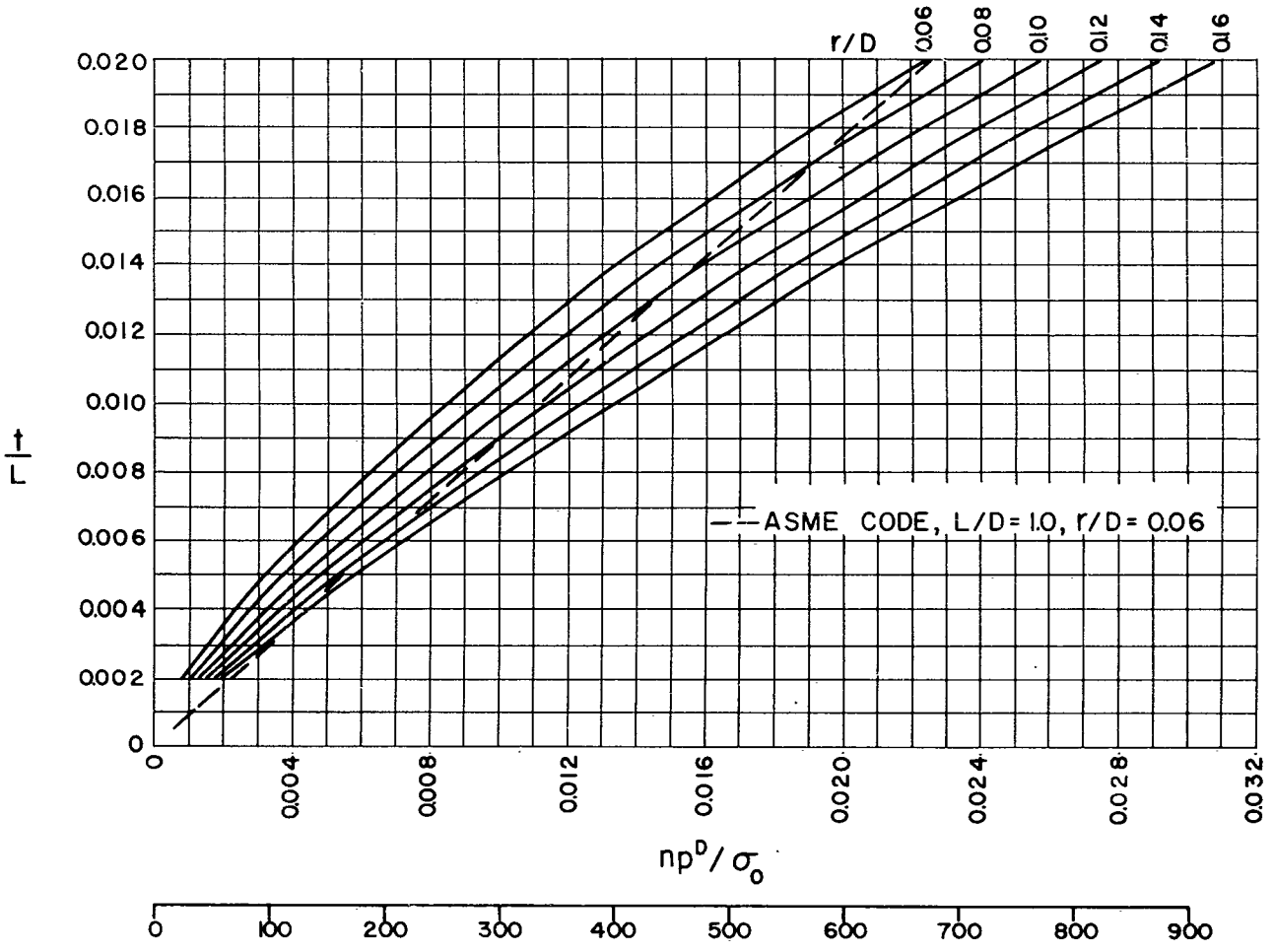

FIG. 8 PLOT OF $\frac{np^D}{\sigma_0} = (0.33 + 5.5\frac{r}{D})\frac{t}{L} + 28(1 - 2.2\frac{r}{D})(\frac{t}{L})^2 - 0.0005$;

np^D/σ_0 MUST NOT EXCEED 2 t/D.